

## Si doping superlattice structure on 6H-SiC(0001)

Lianbi Li<sup>1, a</sup>, Yuan Zang<sup>2</sup> and Jichao Hu<sup>2</sup>

<sup>1</sup>School of Science, Xi'an Polytechnic University, Xi'an 710048, China

<sup>2</sup>Department of Electronic Engineering, Xi'an University of Technology, Xi'an 710048, China

**Abstract.** Si-DSL structures multilayers are prepared on 6H-SiC(0001) successfully. The energy offsets of the n-Si/n-6H-SiC heterojunction in the conduction band and valance band are 0.21eV and 1.65eV, respectively. TEM characterizations of the p/n-Si DSL confirms the epitaxial growth of the Si films with [1-11] preferred orientation and the misfit dislocations with a Burgers vector of  $1/3 \langle 21-1 \rangle$  at the p-Si/n-Si interface. J-V measurements indicate that the heterostructure has apparent rectifying behavior. Under visible illumination with light intensity of 0.6W/cm<sup>2</sup>, the heterostructure demonstrates significant photoelectric response, and the photocurrent density is 2.1mA/cm<sup>2</sup>. Non-UV operation of the SiC-based photoelectric device is realized.

### 1 Introduction

SiC is a desirable material for power devices due to its superior physical properties such as wide bandgap, high thermal conductivity, and high critical electric field, etc..[1-3] However, because of the wide bandgap, SiC-based photoelectric devices can only be driven by ultraviolet (UV) light, which essentially limit its application for a detection of visible and infrared light. Moreover, UV light is harmful to the human body and is not the conventional light source in optical communications. In order to realize non-UV operation, Si film grown on SiC is used as a non-UV light-absorption layer[4, 5], so as to develop the SiC-based photoelectric devices applied in high temperature and high power regions.

At present, the SiC-based Si/SiC heterojunction is comparatively less studied[6-9], and the studies just focused on using Si/SiC heterostructure to improve the performance of the SiC SBD[7], or using Si/SiC heterostructure to solve the problem of SiC/SiO<sub>2</sub> interface defect states in SiC MOSFET[8, 9], the non-UV photoelectric applications of the Si/SiC heterostructure are rarely reported. In our previous work, it was found that the Si/SiC heterojunctions are sensitive to the long-wave length lights ranging from visible to infrared region of the optical spectrum[4, 5]. However, because of the large lattice mismatch between Si and 6H-SiC (~19.6%), there are high density of structural defects such as edge misfit dislocations at the hetero-interface[10], stacking faults and twins in Si films[11], which led to a small carrier lifetime and poor device properties[4]. The doping superlattice (DSL) is a structure composed of the periodic p/n doped layers. In doping superlattice structures, the space charge potential of ionized impurities modulates

the bandgaps of the materials, separates the electrons and holes spatially and thus enhances the carrier lifetime and the photoelectric properties. The DSL structures based on amorphous hydrogenated Silicon (a-Si:H) are investigated[12, 13]. Compared to the unstructured a-Si:H, up to tenfold increase of the photoconductivity is observed.

In this paper, p/n-Si DSL structures on 6H-SiC substrates were adopted to promote the photoelectric properties of the Si/SiC heterojunctions. The non-UV photodetector with the DSL structure was fabricated on 6H-SiC by low-pressure chemical vapor deposition (LPCVD). Transmission electron microscopy (TEM) and selected area electron diffraction (SAED) were employed to investigate the interface structure of Si-DSL/SiC heterojunction, and the photoelectric characteristics were investigated.

### 2 Experimental

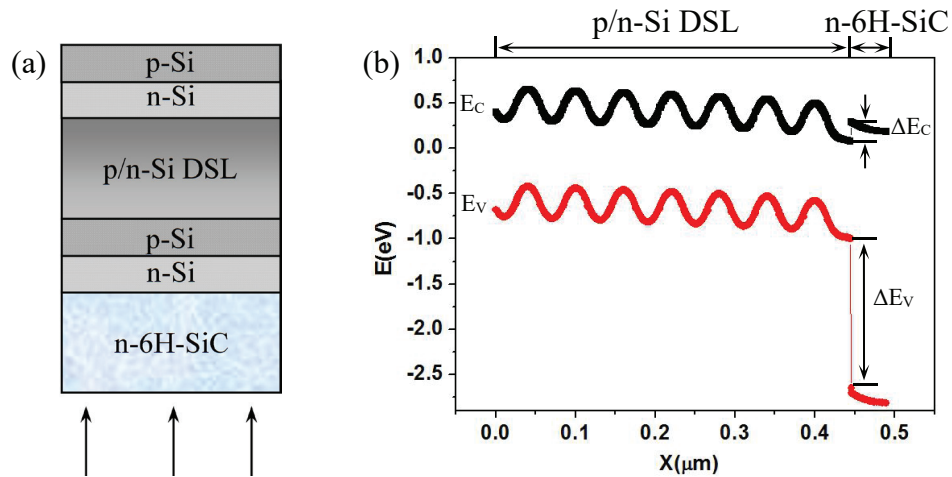
p/n-Si DSL structures are grown on n-type 6H-SiC(0001) Si-face by LPCVD. An n-type doped (impurity concentration of  $\sim 10^{17} \text{cm}^{-3}$ ) 6H-SiC(0001) wafer with a thickness of 300  $\mu\text{m}$  was purchased from II-VI Inc.. Silane (SiH<sub>4</sub>), diborane (B<sub>2</sub>H<sub>6</sub>) and hydrogen (H<sub>2</sub>) are used as a silicon source, a p-type doping source and a carrier, respectively. After the standard RCA cleaning processes[15], 6H-SiC substrates were treated in high-purity H<sub>2</sub> at 1050 °C for 10min. And then the p/n-Si DSL structures were prepared at 900 °C. To prepare the ohmic contacts, Al electrodes on Si and Ni electrodes on 6H-SiC are prepared by magnetron sputtering followed by annealing at 900 °C and 1050 °C, respectively.

<sup>a</sup> Corresponding author: xpu\_lilianbi@163.com

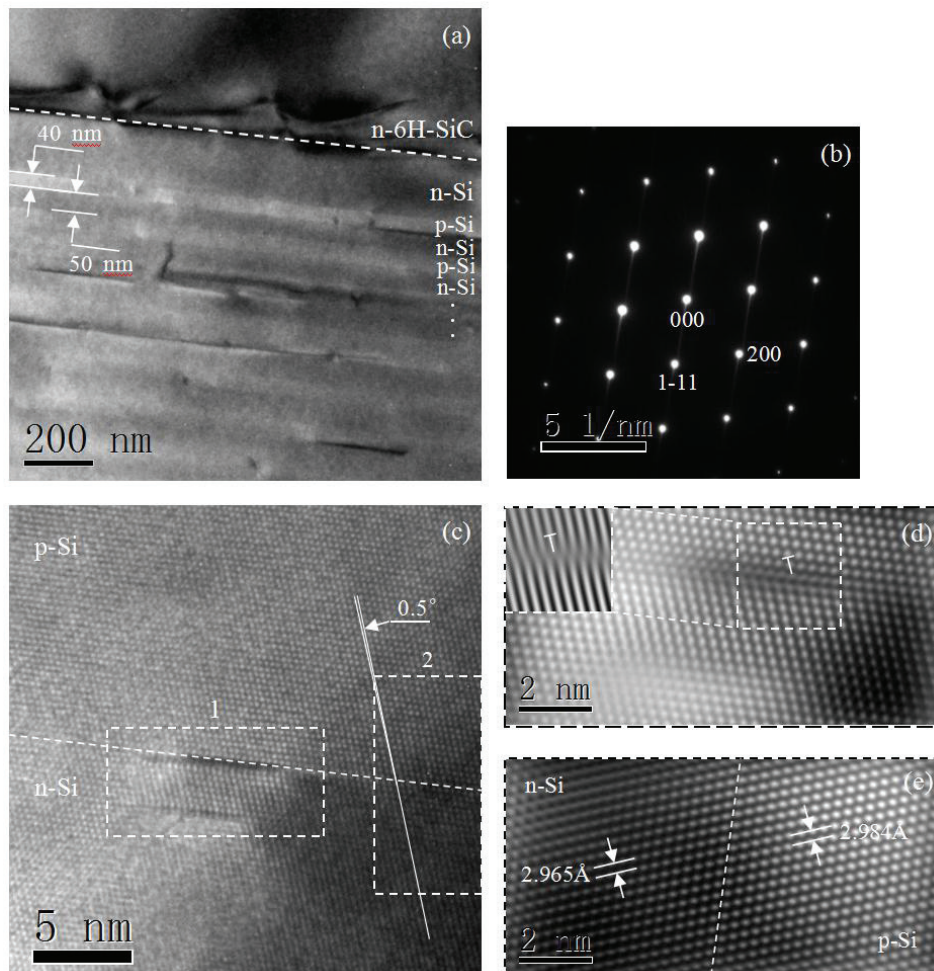
### 3 Results and discussion

Figure 1(a) shows the schematic diagram of Si-DSL/6H-SiC heterostructure. Because 6H-SiC can be used as the penetration window of the visible and near-infrared lights, the light irradiated from the 6H-SiC side in photoelectric test. As is well known, when light is from the high energy bandgap side (6H-SiC), photons of energy between the two energy band gaps (wavelength range from 400nm to 1100nm), pass freely through the

wide gap side and are absorbed in the low-energy bandgap material side (Si). The photoelectric characteristics of Si-DSL/6H-SiC heterostructure are simulated by Silvaco-TCAD. In simulation, the bandgap and electron affinity of 6H-SiC are set as 3.0eV and 3.85eV[14], respectively. The impurity concentrations of the n-Si and p-Si layers are set as  $10^{15}\text{cm}^{-3}$  and  $10^{16}\text{cm}^{-3}$ . The impurity concentration of n-type 6H-SiC with a thickness of 300  $\mu\text{m}$  is  $10^{17}\text{cm}^{-3}$ , which are consistent with the experimental parameters. Figure 1(b) shows the



**Fig.1** Schematic diagram (a) and energy band diagram (b) of Si doping superlattice structure on 6H-SiC in a thermal equilibrium state.  $\Delta E_c=0.21\text{eV}$ ,  $\Delta E_v=1.65\text{eV}$ . The arrows indicate the incident direction of the light.



**Figure 2** TEM and SAED images of the Si-DSL/6H-SiC heterostructure. (a) Cross-sectional low magnification TEM image, (b) SAED patterns of the Si films, (c) HRTEM image of the p/n-Si doping superlattice interface, and the processed HRTEM images of region 1(d) and region 2 (e) by using FFT and Fourier mask filtering technique.

energy band diagram of p/n-Si DSL structures on 6H-SiC in a thermal equilibrium state. It is shown that there are energy offsets of the n-type isotype Si/6H-SiC heterostructure in the conduction band  $\Delta E_C$  and valence band  $\Delta E_V$ , which are about 0.21eV and 1.65eV, respectively. The electron affinity of poly-Si (~4.05eV) is close to that of 6H-SiC, which possibly makes the electron barrier height of the Si/6H-SiC heterostructure very low. The electrons are the dominated current carriers because of the lower electron barrier.

The low magnification cross-sectional TEM bright-field image of the Si-DSL/6H-SiC heterostructure is shown in Fig. 2(a). In this image, the upper part belongs to the 6H-SiC substrate, while the lower part represents the p/n-Si DSL structures. The Si-DSL structures with obvious contrast differences show 40nm-p-Si/50nm-n-Si multilayers are prepared on 6H-SiC(0001) Si-face successfully. The interface of the p/n-Si DSL is abrupt in structure. The SAED patterns of the p/n-Si DSL corresponding to Si[011] zone axes are shown in Fig. 2(b), confirming the epitaxial growth of the Si films with [1-11] preferred orientation. Figure 2(c) shows a high-resolution TEM image of the p-Si/n-Si interface. There are some structural defects at the interface. The [111] direction was tilted by  $0.5^\circ$  at the interface. Fourier filtering technique (FFT) is applied to reveal the periodic atomic arrangement of the p/n-Si DSL interface. Figure 2(d) shows the FFT image of region 1 in Fig. 2(c). It is shown that relatively small amounts of misfit dislocations (MD, indicated by the arrows) appear at the p-Si/n-Si interface, which can be easily identified by extra lattice fringes in p-Si layer. The MDs are of the pure edge type with a Burgers vector of  $1/3 \langle 21-1 \rangle$  parallel to the interface, which are labeled in Fig. 2(d). Moreover, the crystal plane spacing of the Si film has relatively obvious change at the p/n-Si DSL interface, as shown in Fig. 2(e). The crystal plane spacing of p-Si is 0.64% lower than n-Si layer. It demonstrates that the occurrence of the interfacial MDs can not accommodate the most of lattice mismatch strain and makes the lattice change at the p/n-Si DSL interface.

Figure 3(a) presents the J-V characteristics of the Si-DSL/6H-SiC heterostructure under dark condition. It is shown that the heterostructure has obvious rectifying characteristics with rectifying ratio up to 40 at  $\pm 5V$ . The turn-on voltage is about 1.2V. J-V characteristics of the fabricated Si-DSL/6H-SiC heterostructure on 6H-SiC under visible illumination of  $0.6 W/cm^2$  are shown in Fig. 3(b). The solid and the dashed curves represent the J-V characteristics measured under dark and illuminated conditions, respectively. The heterostructure demonstrates apparent photoelectric behavior, the short-circuit current density  $J_{SC}$  is about  $2.1 mA/cm^2$ . After stopping the visible illumination, the J-V curve immediately returned to the identical one under dark. Non-UV operation of the SiC-based photoelectric device is realized.

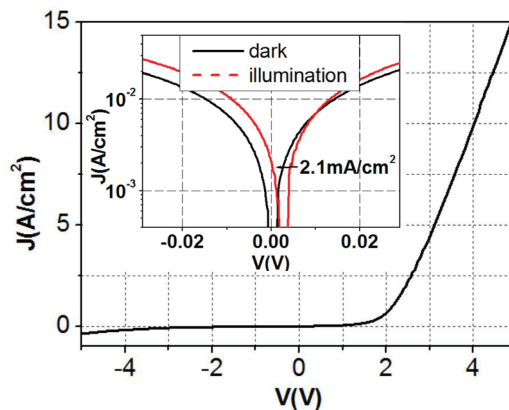


**Figure 3** The electrical and photoelectrical characteristics of the p/n-Si DSL structures on 6H-SiC

## 4 Conclusion

In this paper, Si-DSL structures with 40nm-p-Si/50nm-n-Si multilayers are prepared on 6H-SiC(0001) Si-face successfully. The energy offsets of the n-Si/n-6H-SiC heterojunction in the conduction band and valence band are found to be 0.21eV and 1.65eV, respectively. The electrons are the dominated current carriers because of the low electron barrier. TEM characterizations of the p/n-Si DSL confirms the epitaxial growth of the Si films with [1-11] preferred orientation and the misfit dislocations with a Burgers vector of  $1/3 \langle 21-1 \rangle$  at the p-Si/n-Si interface. Under visible illumination with light intensity of  $0.6 W/cm^2$ , the heterostructure demonstrates significant photoelectric response, and the photocurrent density is  $2.1 mA/cm^2$ . Non-UV operation of the SiC-based photoelectric device is realized.

## Acknowledgements

This work was Supported financially by the National Natural Science Foundation of China (Grant No. 51402230, 21503153), the Project Supported by Natural Science Basic Research Plan in Shaanxi Province of China (Grant No. 2015JM6282), Scientific Research Program Funded by Shaanxi Provincial Education Department (Grant No. 14JK1302) and China Postdoctoral Science Foundation funded project (Grant No. 2013M532072).

## References

1. J. Hu, X. Xin, J.H. Zhao, F. Yan, B. Guan, J. Seely, B. Kjornrattanawanich, *Opt. Lett.* **31**, 1591 (2006).
2. W.T. Liu, Z.M. Chen, *Power Electronics* **45**, 89 (2011).
3. L.B. Li, Z.M. Chen, Z.Q. Ren, Z.J. Gao, *Chin. Phys. Lett.* **30**, 097304 (2013).
4. L.B. Li, Z.M. Chen, W.T. Liu, W.C. Li, *Electron. Lett.* **48**, 1227 (2012).

5. H. Tetsuya, T. Hideaki, S. Yoshio, T. Satoshi, H. Masakatsu, *Mater. Sci. Forum*, **483 - 485**, 953 (2005).
6. A. Pérez-Tomás, M.R. Jennings, M. Davis, J.A. Covington, P.A. Mawby, V. Shah, T. Grasby, *J. Appl. Phys.* **102**, 014505 (2007).
7. A. Pérez-Tomás, M.R. Jennings, M. Davis, V. Shah, T. Grasby, J.A. Covington, P.A. Mawby, *Microelectron. J.* **38**:1233 (2007).
8. O.J. Guy, T.E. Jenkins, M. Lodzinski, A. Castaing, S.P. Wilks, P. Bailey, T.C.Q. Noakes, *Mater. Sci. Forum* **556 - 557**, 509 (2007).
9. L. B. Li, Z. M. Chen, Y. Zang, S. Feng, *Mater. Lett.* **163**, 47 (2016).
10. L. B. Li, Z. M. Chen, Y. Zang, *CrystEngComm* **18**, 5681 (2016).
11. J. Kakalios, H. Fritzsche, *Phys. Rev. Lett.* **53**, 1602 (1984).
12. M. Hundhausen, L. Ley, R. Carius, *Phys. Rev. Lett.* **53**, 1598 (1984).
13. Tokuyuki Teraji, Shiro Hara. Control of interface states at metal/6H-SiC(0001) interfaces, *Phys. Rev. B* **70**, 035312 (2004).
14. W. Kern and D. A. Puotinen, *RCA Rev.* **31**, 187 (1970).